TDA Progress Report 42-123

November 15, 1995

6340

P 30

Optimum Detection of Tones Transmitted by a Spacecraft

M. K. Simon and M. M. Shihabi
Communications Systems and Research Section

T. Moon[1]
Utah State University, Logan, Utah

The performance of a scheme proposed for automated routine monitoring of deep-space missions is presented. The scheme uses four different tones (sinusoids) transmitted from the spacecraft (S/C) to a ground station with the positive identification of each of them used to indicate different states of the S/C. Performance is measured in terms of detection probability versus false alarm probability with detection signal-to-noise ratio as a parameter. The cases where the phase of the received tone is unknown and where both the phase and frequency of the received tone are unknown are treated separately. The decision rules proposed for detecting the tones are formulated from average-likelihood ratio and maximum-likelihood ratio tests, the former resulting in optimum receiver structures.

I. Introduction

It has been proposed that automated routine monitoring of deep-space missions be provided by transmitting one out of n (typically $n = 4$) different subcarriers (tones) from the spacecraft (S/C) and then using a small automated terminal (for example, a 6-m low Earth orbiter terminal (LEO-T)-class) ground station to detect the presence or absence of each possible tone. The positive identification of each of the tones at the receiver will indicate different stages of the S/C, for example, S/C healthy, S/C needs help, S/C is going to transmit telemetry, etc. Since each of these tones is transmitted from the S/C to the ground over an additive white Gaussian noise (AWGN) channel along with the added possibility of Doppler distortion, the above-mentioned detection problem to be solved at the receiver can be formulated as a binary hypotheses test of signal plus noise versus noise only. In the most general case, the signal is modeled as a constant power sinusoid with unknown [i.e., uniformly distributed on $(-\pi, \pi)$] phase and unknown (i.e., uniformly distributed in some interval (f_1, f_2) governed by the amount of Doppler) frequency.

The optimum solution to problems of this nature is based upon maximum-likelihood (ML) considerations of the type discussed in VanTrees [1]. In particular, the solution takes the form of a binary hypothesis likelihood ratio test against a threshold whose value depends on the specified false alarm and detection probabilities, the available signal power-to-noise spectral density ratio, and the duration of

[1] This work was performed under a NASA Summer Faculty Fellowship at the Jet Propulsion Laboratory, Communications Systems and Research Section.

the observation of the hypotheses. We shall see that there are, in principle, two detection/estimation philosophies suggested by the ML approach, corresponding respectively to what is commonly known as *noncoherent* detection, wherein no attempt is made to estimate the unknown parameters prior to detection, and *pseudocoherent* detection, wherein an attempt is made to first estimate the parameters (using an ML approach) and then to use these estimates to aid in the detection process [2]. Since there appears to be some question about which is the better approach, we shall consider both approaches, discuss their philosophical differences, and compare their performances.

This article is organized in two parts. In Part 1, we consider the problem of optimally detecting a sinusoidal signal of known amplitude (power) and frequency but of unknown phase [i.e., uniformly distributed on $(-\pi, \pi)$] transmitted from a S/C to the ground over an AWGN channel. In so far as the optimum receiver design is concerned, the problem will be formulated as a binary hypothesis test of signal plus noise versus noise only with a single unknown parameter (i.e., carrier phase). In Part 2, we consider the added possibility of Doppler distortion, which produces an uncertainty in the received carrier frequency. Once again, the problem can be formulated as a binary hypothesis test of signal plus noise versus noise only, where now the signal is modeled as a constant power sinusoid with unknown phase and unknown frequency. Unfortunately, however, the theory for this case is not as well developed in [1] as for the case where frequency is known. Nevertheless, other researchers [3–6] have examined problems of this type in the context of frequency-hopped (FH) or direct sequence (DS) spread spectrum communication systems, and we shall make use of their results wherever appropriate.

Part 1. Known Frequency and Unknown Phase

II. The Average-Likelihood Ratio Test

A. Derivation of the Optimum Decision Rule and Associated Receiver Structure

Consider the transmission of a fixed (known) amplitude sinusoid with known frequency and unknown phase over an AWGN channel. As such, the received signal can be modeled over the interval of observation $0 \leq t \leq T$ as corresponding to either of two hypotheses, namely,

$$r(t) = s(t, \theta) + n(t) = \sqrt{2P}\cos(\omega_c t + \theta) + n(t) \tag{1a}$$

when indeed the signal was sent (hypothesis H_1) or

$$r(t) = n(t) \tag{1b}$$

when the signal was not sent (hypothesis H_0). In Eq. (1a), P, ω_c respectively denote the known signal power and radian carrier frequency, and θ denotes the unknown carrier phase assumed to be uniformly distributed in the interval $(-\pi, \pi)$. Also, $n(t)$ denotes the AWGN with single-sided power spectral density N_0 W/Hz.

The optimum detection of a signal transmitted over an AWGN channel is the solution to the problem of finding the likelihood ratio (LR), defined as the ratio of the conditional probability density functions (pdf's) of the received signal under the two hypotheses, namely,

$$\Lambda(r(t)) \triangleq \frac{p\,(r(t)|H_1)}{p\,(r(t)|H_0)} \tag{2}$$

and then comparing this ratio to a suitable chosen threshold to decide between H_1 and H_0, i.e.,

$$\Lambda(r(t)) \underset{H_0}{\overset{H_1}{\gtrless}} \eta \tag{3}$$

In the case where *all* parameters of the signal are known, the evaluation of the numerator and denominator of Eq. (2) is straightforward, namely,

$$\begin{aligned} p\left(r(t)|H_1\right) &= \frac{1}{\sqrt{\pi N_0}} \exp\left\{-\frac{1}{N_0}\int_0^T (r(t)-s(t))^2 dt\right\} \\ p\left(r(t)|H_0\right) &= \frac{1}{\sqrt{\pi N_0}} \exp\left\{-\frac{1}{N_0}\int_0^T r^2(t) dt\right\} \end{aligned} \tag{4}$$

When the signal has an unknown parameter, e.g., the phase θ, then to compute the numerator of Eq. (3), we must first condition the pdf $p\left(r(t)|H_1\right)$ on the unknown parameter (θ) and then average over this parameter, i.e.,

$$p\left(r(t)|H_1\right) = \int_{-\pi}^{\pi} p\left(r(t)|H_1,\theta\right) p_\theta(\theta) d\theta \tag{5}$$

where $p_\theta(\theta)$ denotes the pdf of the unknown parameter θ. In our situation, the phase is assumed to be completely unknown and, thus, $p_\theta(\theta)$ is a uniform distribution. Also note that this conditioning on the unknown parameter is now necessary in the denominator of Eq. (3) since the signal does not explicitly appear in $p(r(t)|H_0)$ [see Eq. (4)]. Hence, combining Eqs. (3) through (5), the average-likelihood ratio (ALR)[2] becomes

$$\begin{aligned} \Lambda(r(t)) &= \frac{\frac{1}{2\pi}\int_{-\pi}^{\pi} p(r(t)|H_1,\theta) d\theta}{p(r(t)|H_0)} = \frac{\frac{1}{2\pi}\int_{-\pi}^{\pi} \frac{1}{\sqrt{\pi N_0}} \exp\left\{-\frac{1}{N_0}\int_0^T (r(t)-s(t,\theta))^2 dt\right\} d\theta}{\frac{1}{\sqrt{\pi N_0}} \exp\left\{-\frac{1}{N_0}\int_0^T r^2(t) dt\right\}} \\ &= \exp\left\{-\frac{PT}{N_0}\right\} \frac{1}{2\pi}\int_{\pi}^{\pi} \exp\left\{\frac{2}{N_0}\int_0^T r(t)s(t,\theta) dt\right\} d\theta \\ &= \exp\left\{-\frac{PT}{N_0}\right\} \frac{1}{2\pi}\int_{-\pi}^{\pi} \exp\left\{\frac{2\sqrt{2P}}{N_0}\int_0^T r(t)\cos(\omega_c t+\theta) dt\right\} d\theta \end{aligned} \tag{6}$$

[2] We shall refer to this formulation as an *average*-likelihood ratio (ALR) test to distinguish it from another (in general, less optimum) approach to be discussed shortly, in which a best (maximum-likelihood) estimate of the unknown parameter is obtained first and then used in the detection process. We shall refer to the latter approach as a *maximum*-likelihood ratio (MLR) test. This vernacular is not standard in the literature. What is important to understand here is that the words *average* and *maximum* refer to the manner in which the unknown parameter is handled, i.e., the *estimation* part of the problem and not the manner in which the decision on the hypothesis is made, i.e., the *detection* part of the problem. We shall be more explicit and mathematically precise about these differences later on in the article.

In arriving at the final result in Eq. (6), we have noted that the term $\exp\left\{-\int_0^T r^2(t)dt/N_0\right\}$ is common to both the numerator and denominator and, thus, cancels, and also that

$$\exp\left\{-\frac{1}{N_0}\int_0^T s^2(t,\theta)dt\right\} = \exp\left\{-\frac{2P}{N_0}\int_0^T \cos^2(\omega_c t+\theta)dt\right\} = \exp\left\{-\frac{PT}{N_0}\right\} \tag{7}$$

assuming $\omega_c T >> 1$, as is typically the case. Defining the in-phase (I) and quadrature (Q) correlations

$$L_c \triangleq \int_0^T r(t)\sqrt{2}\cos\omega_c t dt$$

$$L_s \triangleq \int_0^T r(t)\sqrt{2}\sin\omega_c t dt$$

then Eq. (6) can be rewritten as

$$\Lambda(r(t)) = \exp\left\{-\frac{PT}{N_0}\right\}\frac{1}{2\pi}\int_{-\pi}^{\pi}\exp\left\{\frac{2\sqrt{P}}{N_0}L\cos(\theta+\alpha)\right\}d\theta = \exp\left\{-\frac{PT}{N_0}\right\}I_0\left(\frac{2\sqrt{P}}{N_0}L\right) \tag{8}$$

where

$$\begin{aligned} L &\triangleq \sqrt{L_c^2+L_s^2} \\ \alpha &\triangleq \tan^{-1}\frac{L_s}{L_c} \end{aligned} \tag{9}$$

Comparing $\Lambda(r(t))$ to a threshold η is equivalent to comparing $\ln\Lambda(r(t))$ to $\ln\eta$. Thus, taking the natural logarithm of Eq. (8), we obtain the equivalent decision rule

$$\ln I_0\left(\frac{2\sqrt{P}}{N_0}L\right) \underset{H_0}{\overset{H_1}{\gtrless}} \ln\eta + \frac{PT}{N_0} \tag{10}$$

Finally, since $\ln I_0(x)$ is a monotonic function of its argument, x, and since PT/N_0 can be absorbed into the decision threshold, then the decision rule of Eq. (10) can be further simplified to

$$\frac{2\sqrt{P}}{N_0}L \underset{H_0}{\overset{H_1}{\gtrless}} \xi \tag{11}$$

or, equivalently,

$$L^2 \underset{H_0}{\overset{H_1}{\gtrless}} \xi^2 \frac{N_0^2}{4P} \triangleq \gamma \tag{12}$$

i.e., the optimum decision of signal present versus signal absent is determined from a comparison of the output of a square-law envelope detector with a normalized threshold, γ, whose value is determined from the specifications on false alarm probability and detection probability (see the next section). An implementation of the decision rule in Eq. (12) is illustrated in Fig. 1.

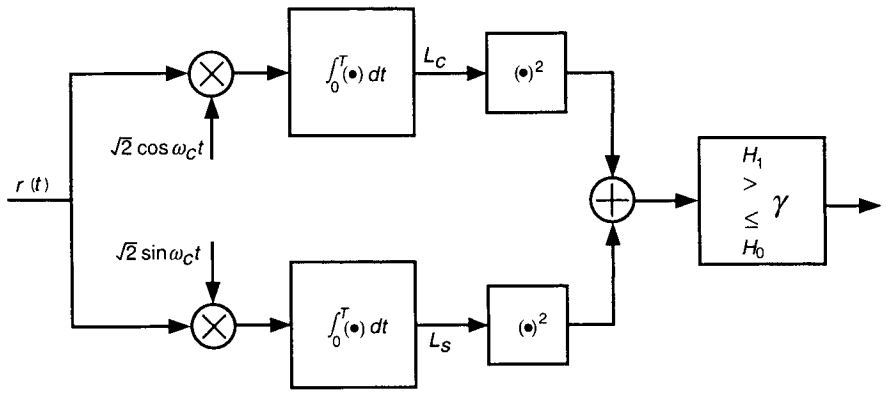

Fig. 1. Average-likelihood (noncoherent) detector for detection of a single sinusoidal tone with known frequency and unknown phase in AWGN.

B. Performance (Receiver Operating Characteristic)

The performance of the receiver in Fig. 1 is described in terms of its *false alarm probability* (P_F), defined as the probability of deciding H_1 (signal is present) when indeed H_0 is true (signal is absent), and its *probability of detection* (P_D), defined as the probability of deciding H_0 (signal is absent) when indeed H_1 is true (signal is present). These probabilities are readily computed from knowledge of the first and second moments of the Gaussian random variables L_c and L_s [see Eq. (8)] under the two hypotheses, namely,

$$\left.\begin{aligned} H_0: \quad & E\{L_c\} = E\{L_s\} = 0 \\ & \text{var}\,\{L_c\} = \text{var}\,\{L_s\} = \frac{N_0 T}{2} \\ H_1: \quad & E\{L_c|\theta\} = \sqrt{PT}\cos\theta \\ & E\{L_s|\theta\} = -\sqrt{PT}\sin\theta \\ & \text{var}\,\{L_c\} = \text{var}\,\{L_s\} = \frac{N_0 T}{2} \end{aligned}\right\} \tag{13}$$

To compute P_F, we observe that, under hypotheses H_0, L is a Rayleigh random variable (L^2 is a central chi-squared random variable). Thus,

$$P_F = Pr\{H_1|H_0\} = Pr\{L^2 > \gamma|H_0\} = \int_0^{2\pi}\int_{\sqrt{\gamma}}^{\infty} \frac{1}{2\pi(N_0T/2)} L\exp\left(-\frac{L^2}{N_0T}\right) dLd\theta$$

$$= \int_{\sqrt{\gamma/N_0T}}^{\infty} 2R\exp(-R^2)dR = \exp\left(-\frac{\gamma}{N_0T}\right) \tag{14}$$

Similarly, we observe that, under hypothesis H_1, L is a Rician random variable (L^2 is a noncentral chi-squared random variable). Thus,

$$\left.\begin{aligned} P_D &= Pr\{H_1|H_1\} = Pr\{L^2 > \gamma|H_1\} = \int_{\sqrt{\gamma}}^{\infty} \frac{1}{N_0T/2} L\exp\left(-\frac{L^2+\beta^2}{N_0T}\right) I_0\left(\frac{2L\beta}{N_0T}\right) dL \\ \beta^2 &\triangleq (E\{L_c|\theta\})^2 + (E\{L_s|\theta\})^2 = PT^2 \\ &= \int_{\sqrt{2\gamma/N_0T}}^{\infty} R\exp\left(-\frac{R^2+d^2}{2}\right) I_0(Rd)dR = Q\left(d, \sqrt{\frac{2\gamma}{N_0T}}\right) \end{aligned}\right\} \tag{15}$$

where

$$d^2 \triangleq \frac{2PT}{N_0} = \frac{2E}{N_0} \tag{16}$$

is the detection signal-to-noise ratio (SNR) and $Q(\alpha, \beta)$ is the Marcum Q-function defined by [1]:

$$Q(\alpha, \beta) = \int_{\beta}^{\infty} z\exp\left(-\frac{z^2+\alpha^2}{2}\right) I_0(\alpha z)dz \tag{17}$$

Combining Eqs. (14) and (15) and eliminating the normalized detection threshold, one obtains the receiver operating characteristic (ROC) given by

$$P_D = Q\left(d, \sqrt{-2\ln P_F}\right) \tag{18}$$

which is illustrated in Fig. 2 for several values of the parameter d (or, equivalently, E/N_0). Alternatively, P_D is plotted versus d^2 with P_F as a parameter in Fig. 3.

III. The Maximum-Likelihood Ratio Test

A. Derivation of the Optimum Decision Rule and Associated Receiver Structure

Although the *exact* evaluation of the numerator of the likelihood ratio in Eq. (2), i.e., $p(r(t)|H_1)$ is obtained from the law of conditional probability as described by Eq. (5), namely, conditioning on the unknown parameter and averaging its distribution, it is also possible to approximate this numerator by first finding the ML estimate of the unknown parameter and then substituting this value into the conditional probability $p(r(t)|H_1, \theta)$. That is, we approximate $p(r(t)|H_1)$ by $p\left(r(t)|H_1, \hat{\theta}_{ML}\right)$, in which case the likelihood ratio test (now referred to as the *maximum*-likelihood ratio (MLR) test) becomes

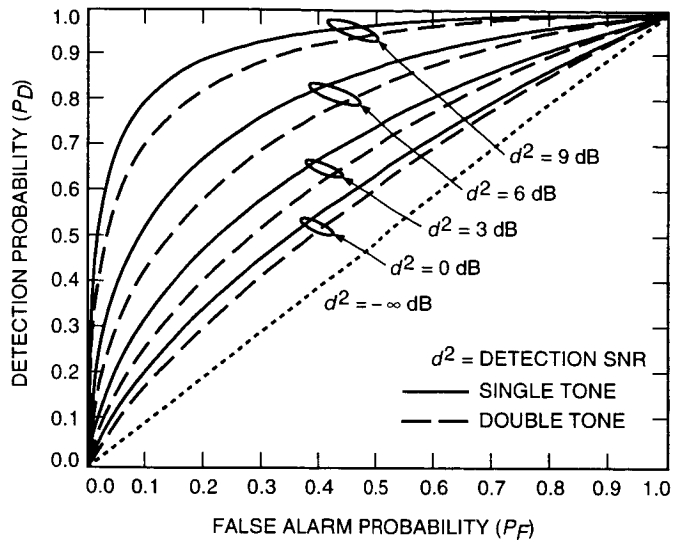

Fig. 2. ROC: frequency known and phase unknown.

$$\Lambda(r(t)) \cong \frac{p\left(r(t)|H_1, \hat{\theta}_{ML}\right)}{p\left(r(t)|H_0\right)} \underset{H_0}{\overset{H_1}{\gtrless}} \eta \tag{19}$$

We refer to this approach of first optimally estimating the phase and then using this estimate to aid the detection process as *pseudocoherent* detection. It is important at this point to emphasize that in the general context of problems of this type, i.e., detection of signals with completely unknown parameters, *the performance of a receiver derived from MLR considerations (e.g., a pseudocoherent receiver) is never better than the performance of the ALR receiver (e.g., a noncoherent receiver), which is indeed optimum under the assumed conditions.* Thus, *at best*, one could hope that the MLR receiver would perform equally well as does the ALR receiver. In the next section, we shall indeed reveal the extent to which this equality in performance can be achieved for the problem at hand. First, however, let us derive the ML estimate of phase, namely, $\hat{\theta}_{ML}$, to be used in approximating the numerator of the likelihood ratio.

The ML estimate of θ is defined as

$$\hat{\theta}_{ML} = \max_{\theta} \frac{p(r(t)|H_1, \theta)}{p(r(t)|H_0)} \tag{20}$$

Using Eq. (4) in Eq. (20), it is straightforward to show that

$$\hat{\theta}_{ML} = \max_{\theta} \exp\left\{\frac{2}{N_0}\int_0^T r(t)s(t,\theta)dt\right\} = \max_{\theta} \exp\left\{\frac{2\sqrt{2P}}{N_0}\int_0^T r(t)\cos(\omega_c t + \theta)\,dt\right\}$$

$$= \max_{\theta} \exp\left\{\frac{2\sqrt{P}}{N_0} L\cos(\theta + \alpha)\right\} \tag{21}$$

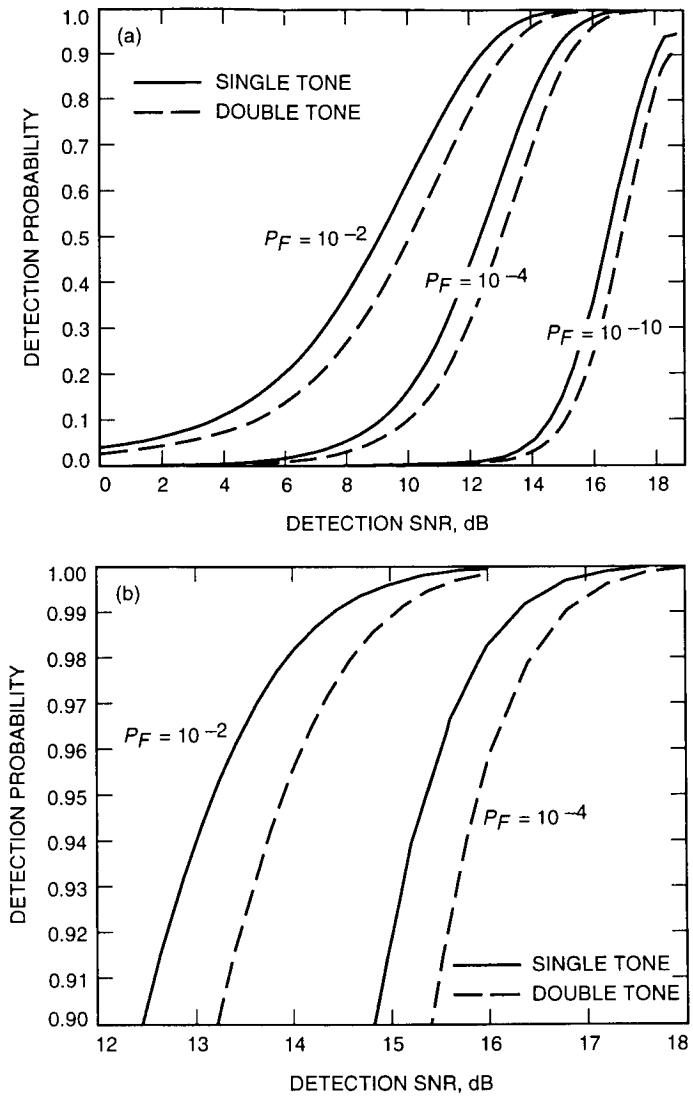

Fig. 3. Detection probability (P_D) versus detection SNR (d^2): (a) frequency known and phase unknown and (b) frequency known and phase unknown (expanded view).

where the envelope, L, and the phase, α, are defined by Eq. (9) together with Eq. (8). Since L is positive and independent of θ, then the maximization required in Eq. (21) is achieved when the argument of the cosine function is equal to zero. Thus,

$$\hat{\theta}_{ML} = -\alpha \tag{22}$$

An implementation of this ML estimator of the unknown channel phase is illustrated in Fig. 4. Also illustrated in Fig. 4 is the pseudocoherent detector that employs this ML phase estimator, which can be obtained by taking the natural logarithm of Eq. (19). We now find the decision rule based on the MLR test in Eq. (19) and compare it with that of the previously discussed ALR test. Using Eq. (22) in Eq. (19) gives, by analogy with Eq. (8),

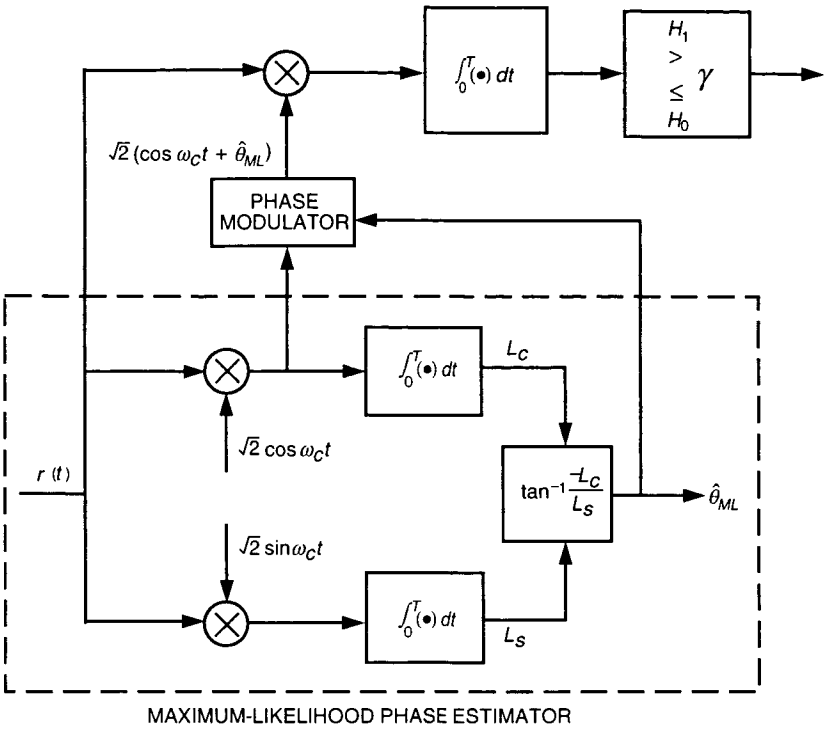

Fig. 4. Maximum-likelihood phase estimator and pseudocoherent detector.

$$\Lambda(r(t)) \cong \exp\left\{-\frac{PT}{N_0}\right\} \exp\left\{\frac{2\sqrt{P}}{N} L \cos\left(\hat{\theta}_{ML} + \alpha\right)\right\} = \exp\left\{-\frac{PT}{N_0}\right\} \exp\left\{\frac{2\sqrt{P}}{N_0} L\right\} \tag{23}$$

Taking the natural logarithm of Eq. (23), we then have, by analogy with Eq. (10),

$$\frac{2\sqrt{P}}{N_0} L \underset{H_0}{\overset{H_1}{\gtrless}} \ln\eta + \frac{PT}{N_0} \tag{24}$$

Since, as previously noted, the term PT/N_0 can be absorbed into the decision threshold, then an equivalent test to Eq. (24) is

$$\frac{2\sqrt{P}}{N_0} L \underset{H_0}{\overset{H_1}{\gtrless}} \xi \tag{25}$$

which is identical to Eq. (11)! Thus, we conclude that in this particular circumstance, *the MLR test (pseudocoherent receiver) and the ALR test (noncoherent receiver) are identical.* Hence, the performance of the pseudocoherent receiver is also described by Figs. 2 and 3. It is to be emphasized again that the equivalence found here between ALR and MLR receivers is not typical and applies only in this very

special case of the detection of a signal with known frequency and unknown phase. More often than not, the receiver derived from the MLR approach will have an inferior performance to the optimum one derived from the ALR approach.

IV. A More Precise Formulation of the Problem

In reality, the subcarriers that are transmitted to indicate the status of the S/C are continuous square waves that biphase modulate the carrier. Thus, denoting the carrier radian frequency and phase by ω_c and θ_c (previously called θ), respectively, and the square-wave subcarrier radian frequency and phase by ω_{sc} and θ_{sc}, respectively, then the received signal analogous to Eq. (1a) is given by

$$\begin{aligned} r(t) &= s(t,\theta_c,\theta_{sc}) + n(t) = \sqrt{2P}\sin\left(\omega_c t + \theta_c + \frac{\pi}{2}\ \mathrm{Sq}\ (\omega_{sc}t + \theta_{sc})\right) + n(t) \\ &= \sqrt{2P}\ \mathrm{Sq}\ (\omega_{sc}t + \theta_{sc})\cos(\omega_c t + \theta_c) + n(t) \end{aligned} \tag{26}$$

Assuming that the harmonics with frequencies other than the sum and difference of ω_c and ω_{sc} are filtered out, then in so far as detection is concerned, we may consider the received signal to be[3]

$$r(t) = s\,(t,\theta_c,\theta_{sc}) + n(t) = \sqrt{P}\,\{\cos[(\omega_c + \omega_{sc})t + (\theta_c + \theta_{sc})] + \cos[(\omega_c - \omega_{sc})t + (\theta_c - \theta_{sc})]\} + n(t) \tag{27}$$

i.e., the problem is to detect the presence or absence of *two* tones in an AWGN background where both ω_c and ω_{sc} are assumed to be known but both θ_c and θ_{sc} are assumed to be completely unknown. For convenience of notation, we shall rewrite Eq. (27) as

$$r(t) = s(t,\theta_+,\theta_-) + n(t) = \sqrt{P}\,\{\cos[\omega_+ t + \theta_+] + \cos[\omega_- t + \theta_-]\} + n(t) \tag{28}$$

where

$$\left.\begin{aligned} \omega_\pm &\triangleq \omega_c \pm \omega_{sc} \\ \theta_\pm &\triangleq \theta_c \pm \theta_{sc} \end{aligned}\right\} \tag{29}$$

At first glance, it might appear that, because the phases θ_c and θ_{sc} appear in the two signal tones as their sum and difference, the detection of these tones cannot be performed independently. Interestingly enough, $\theta_+ \triangleq \theta_c + \theta_{sc}$ and $\theta_- \triangleq \theta_c - \theta_{sc}$ when reduced modulo 2π can be shown to be independent uniformly distributed random variables (see the Appendix). Thus, as we shall see shortly, the detection of two distinct sinusoidal tones with independent random phases in an AWGN background can be treated by a likelihood ratio approach analogous to that discussed in the previous section for a single tone in the same background.

[3] In reality, the $\sqrt{P}$ amplitude factor in Eq. (27) should be $(2\sqrt{2}/\pi)\sqrt{P} = 0.9003\sqrt{P}$ to account for the amplitude of the first harmonic in the square-wave subcarrier. For simplicity, we shall ignore this minor difference.

A. The ALR Test

As discussed in Section II, the optimum decision rule is, in general, obtained by applying the *average*-likelihood approach, which in this case means averaging the conditional likelihood function over the *two* random phases θ_+ and θ_-. In particular, the conditional pdf of the received signal under hypothesis H_1 is analogous to Eq. (5):

$$p(r(t|H_1) = \int_{-\pi}^{\pi}\int_{-\pi}^{\pi} p(r(t)|H_1,\theta_+,\theta_-)p_{\theta_+,\theta_-}(\theta_+,\theta_-)d\theta_+ d\theta_- = \left(\frac{1}{2\pi}\right)^2 \int_{-\pi}^{\pi}\int_{-\pi}^{\pi} p(r(t)|H_1,\theta_+,\theta_-)d\theta_+ d\theta_- \tag{30}$$

and, hence, the ALR becomes

$$\begin{aligned}\Lambda(r(t)) &= \frac{\left(\frac{1}{2\pi}\right)^2 \int_{-\pi}^{\pi}\int_{-\pi}^{\pi} p(r(t)|H_1,\theta_+,\theta_-)d\theta_+ d\theta_-}{p(r(t)|H_0)} \\ &= \exp\left\{-\frac{PT}{N_0}\right\}\left(\frac{1}{2\pi}\right)^2 \int_{-\pi}^{\pi} \exp\left\{\frac{2\sqrt{P}}{N_0}\int_0^T r(t)\cos(\omega_- t+\theta_-)dt\right\} d\theta_- \\ &\quad \times \int_{-\pi}^{\pi} \exp\left\{\frac{2\sqrt{P}}{N_0}\int_0^T r(t)\cos(\omega_+ t+\theta_+)dt\right\} d\theta_+ \end{aligned} \tag{31}$$

Defining the I and Q correlations for the sum and difference frequencies by

$$\left.\begin{aligned} L_{c\pm} &\triangleq \int_0^T r(t)\sqrt{2}\cos\omega_\pm t dt \\ L_{s\pm} &\triangleq \int_0^T r(t)\sqrt{2}\sin\omega_\pm t dt \end{aligned}\right\} \tag{32}$$

then, the likelihood function of Eq. (30) can be rewritten as

$$\Lambda(r(t)) = \exp\left\{-\frac{PT}{N_0}\right\} I_0\left(\frac{\sqrt{2P}}{N_0}L_-\right) I_0\left(\frac{\sqrt{2P}}{N_0}L_+\right) \tag{33}$$

where, analogous to Eq. (9), the envelopes corresponding to the upper and lower subcarrier tones are given by

$$L_\pm \triangleq \sqrt{L_{c\pm}^2 + L_{s\pm}^2} \tag{34}$$

Alternately, in terms of the log-likelihood function, we arrive at the decision rule

$$\ln I_0\left(\frac{\sqrt{2P}}{N_0}L_-\right) + \ln I_0\left(\frac{\sqrt{2P}}{N_0}L_+\right) \underset{H_0}{\overset{H_1}{\gtrless}} \ln\eta + \frac{PT}{N_0} \tag{35}$$

Note that now, despite the fact that $\ln I_0(x)$ is a monotonic function of its argument, x, we cannot directly simplify Eq. (35) to a form analogous to Eq. (11). Rather, to get such a form, one must approximate the $\ln I_0(x)$ function by its series and asymptotic forms for small and large arguments, namely,

$$\ln I_0(x) \cong \begin{cases} \dfrac{x^2}{4}, & \text{small } x \\ |x|, & \text{large } x \end{cases} \tag{36}$$

Thus, for example, if we invoke the small argument approximation of the $\ln I_0(x)$ function in Eq. (35), we get the decision rule (optimum for small SNR)

$$L_-^2 + L_+^2 \triangleq L^2 \underset{H_0}{\overset{H_1}{\gtrless}} \gamma \tag{37}$$

where γ is again a normalized threshold [not necessarily equal to the one defined in Eq. (12)]. The decision rule in Eq. (37) suggests the ALR structure illustrated in Fig. 5, which is analogous to that given in Fig. 1. For the large argument approximation of the $\ln I_0(x)$ function, the implementation of Fig. 5 would require square root devices in each arm entering the final summer prior to the decision device.

B. The MLR Test

Let us now again compare the noncoherent two-tone detector derived from ALR considerations and specified by the decision rule of Eq. (35) to a pseudocoherent detector that can be derived from MLR considerations. In particular, consider the joint ML estimates $\hat{\theta}_{ML+}, \hat{\theta}_{ML-}$ of θ_+, θ_- defined as

$$\hat{\theta}_{ML+}, \hat{\theta}_{ML-} = \max_{\theta_+,\theta_-} \frac{p(r(t)|H_1, \theta_+, \theta_-)}{p(r(t)|H_0)} \tag{38}$$

which, because of the independence of θ_+ and θ_-, is determined as

$$\begin{aligned} \hat{\theta}_{ML+}, \hat{\theta}_{ML-} &= \max_{\theta_+,\theta_-} \exp\left\{\frac{2\sqrt{P}}{N_0}\int_0^T r(t)\cos(\omega_- t + \theta_-)dt\right\} \exp\left\{\frac{2\sqrt{P}}{N_0}\int_0^T r(t)\cos(\omega_+ t + \theta_+)dt\right\} \\ &= \max_{\theta_+,\theta_-} \left\{\frac{\sqrt{2P}}{N_0}L_-\cos(\theta_- + \alpha_-)\right\} \exp\left\{\frac{\sqrt{2P}}{N_0}L_+\cos(\theta_+ + \alpha_+)\right\} \end{aligned} \tag{39}$$

where $\alpha_\pm$ are defined in terms of $L_\pm$, analogous to Eq. (9). The solution to Eq. (39) is

$$\hat{\theta}_{ML\pm} = -\alpha_\pm \tag{40}$$

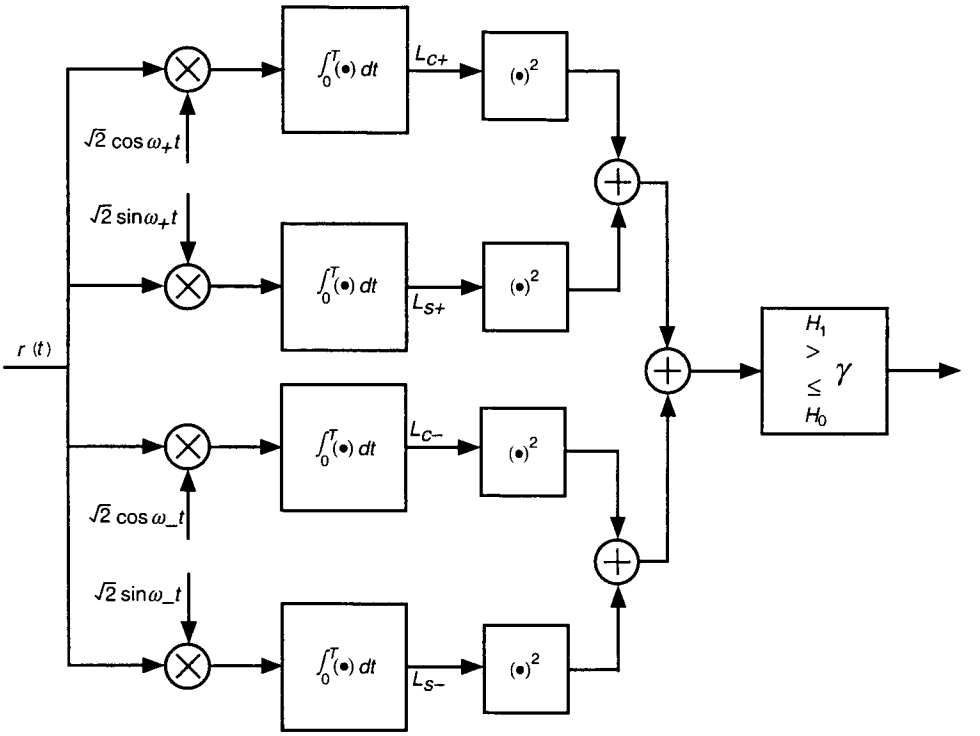

Fig. 5. Average-likelihood (noncoherent) detector for detection of a pair of independent sinusoidal tones with known frequencies and unknown phases in AWGN.

which, when substituted in Eq. (39), gives

$$\Lambda(r(t)) \cong \exp\left\{-\frac{PT}{N_0}\right\} \exp\left\{\frac{\sqrt{2P}}{N_0} L_+\right\} \exp\left\{\frac{\sqrt{2P}}{N_0} L_-\right\} = \exp\left\{-\frac{PT}{N_0}\right\} \exp\left\{\frac{2\sqrt{P}}{N_0} L\right\} \tag{41}$$

Taking the natural logarithm of Eq. (40), we get the decision rule

$$\frac{\sqrt{2P}}{N_0}(L_+ + L_-) \underset{H_0}{\overset{H_1}{\gtrless}} \ln\eta + \frac{PT}{N_0} \tag{42}$$

Comparing Eq. (42) with Eq. (35), we observe that, in the two-tone case, the MLR test (which would lead to a pseudocoherent form of detector analogous to Fig. 4) is *not* the same as the ALR test. However, using the large argument approximation of the $\ln I_0(x)$ function as given by Eq. (36), we see that the ALR and MLR tests once again become equivalent. In summary then, we observe that, *for detection of a single tone in AWGN, the ALR (noncoherent) test and MLR (pseudocoherent) test are equivalent for all SNRs, whereas for the detection of a pair of equal power tones in AWGN, the ALR and MLR tests are equivalent only at sufficiently large SNR.*

C. Performance (Receiver Operating Characteristic)

The performance of the low SNR receiver in Fig. 5 is, as before, described in terms of its false alarm probability (P_F) and its probability of detection (P_D). These probabilities are readily computed from

knowledge of the first and second moments of the Gaussian random variables $L_{c\pm}$ and $L_{s\pm}$ [see Eq. (31)] under the two hypotheses, namely,

$$\left.\begin{aligned} H_0: \quad & E\{L_{c\pm}\} = E\{L_{s\pm}\} = 0 \\ & \text{var}\,\{L_{c\pm}\} = \text{var}\,\{L_{s\pm}\} = \frac{N_0 T}{2} \\ H_1: \quad & E\{L_{c\pm}|\theta\} = \sqrt{\frac{P}{2}} T \cos\theta_{\pm} \\ & E\{L_{s\pm}|\theta\} = \sqrt{\frac{P}{2}} T \sin\theta_{\pm} \\ & \text{var}\,\{L_{c\pm}\} = \text{var}\,\{L_{s\pm}\} = \frac{N_0 T}{2} \end{aligned}\right\} \tag{43}$$

To compute P_F, we observe as before that, under hypothesis H_0, L^2 is a central chi-squared random variable (now with two more degrees of freedom). Thus,

$$P_F = \Pr\{H_1|H_0\} = \Pr\{L^2 > \gamma|H_0\} = \int_{\gamma/N_0T}^{\infty} r\exp(-r)dr = \left(1 + \frac{\gamma}{N_0T}\right)\exp\left(-\frac{\gamma}{N_0T}\right) \tag{44}$$

Similarly, we observe that, under hypothesis H_1, L^2 is a noncentral chi-squared random variable (now with two more degrees of freedom). Thus,

$$P_D = \Pr\{H_1|H_1\} = \Pr\{L^2 > \gamma|H_1\} = \int_{\sqrt{2\gamma/N_0T}}^{\infty} R\left(\frac{R}{d}\right)\exp\left(-\frac{R^2+d^2}{2}\right) I_1(Rd)dR = Q_2\left(d, \sqrt{\frac{2\gamma}{N_0T}}\right) \tag{45}$$

where d^2 is the detection SNR defined as before [see Eq. (16)] and $Q_M(\alpha,\beta)$ is the generalized Marcum Q-function defined by

$$Q_M(\alpha,\beta) = \int_{\beta}^{\infty} z\left(\frac{z}{\alpha}\right)^{M-1}\exp\left(-\frac{z^2+\alpha^2}{2}\right) I_{M-1}(\alpha z)dz \tag{46}$$

Note that $Q_M(\alpha,\beta)$ can be obtained from $Q(\alpha,\beta) \triangleq Q_1(\alpha,\beta)$ by the relation [2, Appendix 5A]

$$Q_M(\alpha,\beta) = Q(\alpha,\beta) + \exp\left(\frac{\alpha^2+\beta^2}{2}\right)\sum_{j=1}^{M-1}\left(\frac{\beta}{\alpha}\right)^j I_j(\alpha\beta)$$

Unfortunately, the normalized detection threshold cannot be explicitly eliminated in Eqs. (39) and (40) to give a closed-form expression for the receiver operating characteristic (ROC) analogous to Eq. (18). However, for any range of interest, the ROC can be determined numerically. Such numerical results are

superimposed on the single-tone detection in Figs. 2, 3(a), and 3(b). We observe that the performance penalty associated with using a pair of subcarrier tones each with half the total power relative to the full-power single carrier tone case is quite small, e.g., on the order of 0.4 dB or less for $P_F = 10^{-2}$ and on the order of 0.3 dB or less for $P_F = 10^{-4}$. The degradation associated with the true optimum ALR scheme as described by the decision rule of Eq. (35) would be even smaller. Thus, the performance curves of the true optimum ALR scheme for two tones would lie between the solid and dashed curves in Figs. 2, 3(a), and 3(b) since indeed these performance results cannot beat those corresponding to the single-tone case. Because of the small degradations involved, we choose not to simulate the true optimum case.

Part 2. Unknown Frequency and Unknown Phase

V. The Average-Likelihood Ratio Test

A. Derivation of the Optimum Decision Rule and Associated Receiver Structure

Consider the transmission of a fixed (known) amplitude sinusoid with unknown frequency and unknown phase over an AWGN channel. Analogous to Eq. (1), the received signal can be modeled over the interval of observation $0 \leq t \leq T$ as corresponding to either of two hypotheses, namely,

$$r(t) = s(t,\theta) + n(t) = \sqrt{2P}\cos(\omega t + \theta) + n(t) \tag{47a}$$

when indeed the signal was sent (hypothesis H_1) or

$$r(t) = n(t) \tag{47b}$$

when the signal was not sent (hypothesis H_0). In addition to the previously defined parameters, in Eq. (47a), $f \triangleq \omega/2\pi$ denotes the unknown carrier frequency assumed to be uniformly distributed in the interval $(f_c - B/2, f_c + B/2)$, where as before f_c denotes the nominal carrier frequency (i.e., in the absence of Doppler). When the signal has two unknown parameters, e.g., the phase θ and frequency f, then to compute the numerator of Eq. (3), we must first condition the pdf $p(r(t)|H_1)$ on *both* of the unknown parameters and then average over them, i.e.,

$$p(r(t)|H_1) = \int_{f_c-B/2}^{f_c+B/2}\int_{-\pi}^{\pi} p(r(t)|H_1,\theta,f)p_\theta(\theta)p_f(f)d\theta df \tag{48}$$

where $p_\theta(\theta), p_f(f)$ respectively denote the pdf's of the unknown parameters θ and f. In our situation, the phase and frequency are assumed to be completely unknown, and thus $p_\theta(\theta)$ and $p_f(f)$ are uniform distributions. Hence, combining Eqs. (3) and (48), the average-likelihood ratio (ALR) becomes

$$\begin{aligned}
\Lambda(r(t)) &= \frac{\dfrac{1}{2\pi B}\displaystyle\int_{f_c-B/2}^{f_c+B/2}\int_{-\pi}^{\pi} p(r(t)|H_1,\theta,f)d\theta df}{p(r(t)|H_0)} \\
&= \exp\left\{-\frac{PT}{N_0}\right\}\frac{1}{2\pi B}\int_{f_c-B/2}^{f_c+B/2}\int_{-\pi}^{\pi}\exp\left\{\frac{2\sqrt{2P}}{N_0}\int_0^T r(t)\cos(\omega_c t+\theta)dt\right\}d\theta df \\
&= \exp\left\{-\frac{PT}{N_0}\right\}\frac{1}{B}\int_{f_c-B/2}^{f_c+B/2} I_0\left(\frac{2\sqrt{P}}{N_0}L(f)\right)df
\end{aligned} \tag{49}$$

where

$$L(f) \triangleq \sqrt{L_c^2(f) + L_s^2(f)} \tag{50}$$

with

$$\left.\begin{aligned} L_c(f) &\triangleq \int_0^T r(t)\sqrt{2}\cos 2\pi f t dt \\ L_s(f) &\triangleq \int_0^T r(t)\sqrt{2}\sin 2\pi f t dt \end{aligned}\right\} \tag{51}$$

It should be noted that $L(f)$ is nothing more than the magnitude of the complex Fourier transform (FT) of $r(t)$ in the interval $0 \leq t \leq T$. If $r(t)$ is band limited to W Hz, then for large WT, the real and imaginary components of this complex FT, namely, $L_c(f), L_s(f)$ can be approximated by the discrete Fourier transforms (DFTs)

$$\left.\begin{aligned} L_c(f) &= \sqrt{2}\frac{1}{2W}\sum_{n=1}^{2WT} r\left(\frac{n}{2W}\right)\cos\left(2\pi f\frac{n}{2W}\right) \\ L_s(f) &= \sqrt{2}\frac{1}{2W}\sum_{n=1}^{2WT} r\left(\frac{n}{2W}\right)\sin\left(2\pi f\frac{n}{2W}\right) \end{aligned}\right\} \tag{52}$$

Comparing $\Lambda(r(t))$ to a threshold produces (after suitable normalization) the ALR decision rule

$$\int_{f_c-B/2}^{f_c+B/2} I_0\left(\frac{2\sqrt{P}}{N_0}L(f)\right) df \underset{H_0}{\overset{H_1}{\gtrless}} \eta \tag{53}$$

Since Eq. (53) is overly demanding to implement, one discretizes the frequency uncertainty interval into $G = B/T^{-1} = BT$ subintervals to each of which is associated a candidate frequency $f_i; i = 0, 1, 2, \cdots, G-1$ located at its center. As such, the integration over the continuous uncertainty region in Eq. (53) is approximated by a discrete (Riemann) sum and, hence, the approximate decision rule becomes

$$\sum_{i=0}^{G-1} I_0\left(\frac{2\sqrt{p}}{N_0}L(f_i)\right) \underset{H_0}{\overset{H_1}{\gtrless}} \eta \tag{54}$$

which has the implementation representation of Fig. 6. It is important to understand that spacing the frequencies $f_i; i = 0, 1, 2, \cdots, G-1$ by $1/T$ guarantees independence of the noise components that appear at the output of each spectral estimate channel. However, orthogonality of the signal components of these same outputs depends on the true value of the received frequency relative to the discretized frequencies $f_i; i = 0, 1, 2, \cdots, G-1$ assumed for implementation of the receiver. That is, if the true received frequency happens to fall on one of the f_i's, then a signal component will appear only in the corresponding spectral

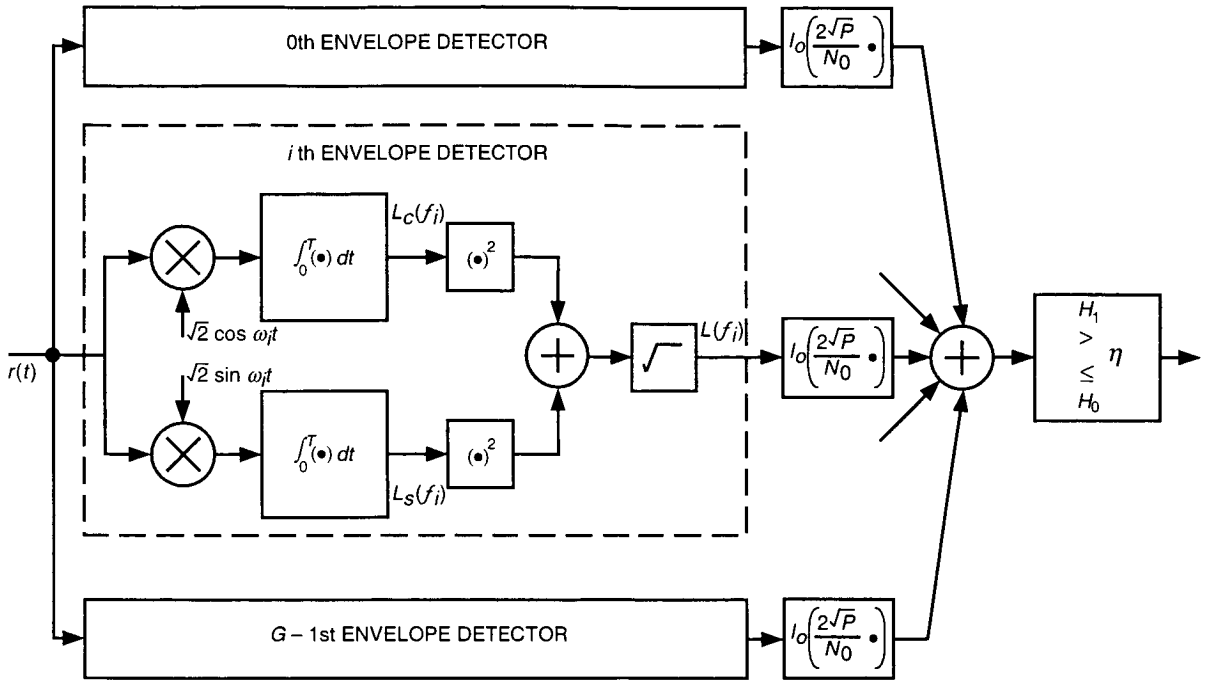

Fig. 6. Average-likelihood (noncoherent) detector for detection of a single sinusoidal tone with unknown frequency and unknown phase in AWGN.

estimate channel, i.e., all other channels will be noise only. On the other hand, if the true received frequency falls somewhere between two of the f_i's, then we have a loss of orthogonality in that a spillover of signal energy occurs in the neighboring spectral estimates. The worst-case spillover would occur when the true received frequency is midway between two of the f_i's.

We conclude this section by noting that a decision metric similar to Eq. (54) arises in the study of FH or DS/low probability of intercept (LPI) optimum ALR (noncoherent) detection [3–5], where in the FH case, $f_i; i - 0, 1, 2, \cdots, G - 1$ corresponds to the G possible frequencies that the transmitted signal can hop to and the detection is based on observation of a single hop of duration $T_H = T$, and in the DS case G is the number of possible code sequences that can occur in the observation interval. Many of the results obtained from these works are directly applicable to the problem at hand.

B. Performance

It is tempting for large values of G (as is typically the case) to apply a central limit theorem argument to the left side of Eq. (11), i.e., approximate it as a Gaussian random variable in so far as computing the receiver operating characteristic associated with this decision rule [4]. Unfortunately, it was shown in [5] that following such an approach is very poor when compared with results obtained from simulation or numerical methods applied to the true decision rule of Eq. (11), even for values of G as large as 1000 or 10,000. In fact, it is stated in [5] that G on the order of "ten thousands is not guaranteed to be large enough to validate the Gaussian approximation." Thus, to obtain the true receiver performance, we too must resort to simulation and/or numerical methods, such as those suggested by Requicha [7], wherein the characteristic function and fast Fourier transforms (FFTs) are used to compute approximate values of the distribution function associated with the left-hand side of Eq. (11). More about this later on.

VI. The Maximum-Likelihood Ratio Test

A. Derivation of the Optimum Decision Rule and Associated Receiver Structure

Although the *exact* evaluation of the numerator of the likelihood ratio in Eq. (2), i.e., $p(r(t)|H_1)$ is obtained from the law of conditional probability as described by Eq. (5), namely, conditioning on the unknown parameters and averaging over their distribution, it is also possible to approximate this numerator by first finding the ML estimates of the unknown parameters and then substituting these values into the conditional probability $p(r(t)|H_1, \theta, f)$. That is, we approximate $p(r(t)|H_1)$ by $p(r(t)|H_1, \hat{\theta}_{ML}, \hat{f}_{ML})$, in which case the likelihood ratio test (now referred to as the *maximum*-likelihood ratio (MLR) test) becomes

$$\Lambda(r(t)) \cong \frac{p\left(r(t)|H_1, \hat{\theta}_{ML}, \hat{f}_{ML}\right)}{p(r(t)|H_0)} \underset{H_0}{\overset{H_1}{\gtrless}} \tag{55}$$

where

$$\hat{\theta}_{ML}, \hat{f}_{ML} \triangleq \max_{\theta, f} \frac{p(r(t)|H_1, \theta, f)}{p(r(t)|H_0)} \tag{56}$$

The maximization over θ required in Eq. (56) can be performed identically to that in Section III [see Eq. (23)]:

$$\max_{\theta} \frac{p(r(t)|H_1, \theta, f)}{p(r(t)|H_0)} = \exp\left(-\frac{PT}{N_0}\right) \exp\left(\frac{2\sqrt{P}}{N_0} L(f)\right) \tag{57}$$

where $L(f)$ is as defined in Eq. (50). Thus, the optimum maximum a posteriori (MAP) decision rule becomes

$$\max_{f} \exp\left(-\frac{PT}{N_0}\right) \exp\left(\frac{2\sqrt{P}}{N_0} L(f)\right) \underset{H_0}{\overset{H_1}{\gtrless}} \eta \tag{58}$$

Since the exponential is a monotonic function of its argument, we have the equivalent decision rule[4]

$$\max_{f} L(f) \underset{H_0}{\overset{H_1}{\gtrless}} \sqrt{\gamma} \tag{59}$$

which results in a *spectral maximum* form of receiver. Again, because of the excessive demand placed on the implementation by the need to evaluate Eq. (59) over a continuum of frequencies, we again quantize the frequency uncertainty interval into $G = BT$ subintervals, each with an associated candidate frequency

[4] We define the normalized threshold equal to $\sqrt{\gamma}$ to be consistent with the notation used in Part 1. In this way, when G is equated to unity, then our results obtained here will reduce to those given in Part 1 for the MLR decision rule.

C-2.

$f_i; i = 0, 1, 2, \cdots, G-1$ located at its center. Thus, the frequency continuous decision rule of Eq. (59) can be approximated by the decision rule

$$\max_i L(f_i) \underset{H_0}{\overset{H_1}{\gtrless}} \sqrt{\gamma} \tag{60}$$

which suggests the receiver of Fig. 7. Here again, as with Eq. (54), the orthogonality of the spectral estimates is not guaranteed unless the frequency of the received signal falls on one of the f_i's. Also, since $L(f_i); i = 0, 1, 2, \cdots, G$ represents a uniform sampling of $L(f)$, then in view of Eq. (52), we can implement Fig. 7 with FFT techniques.

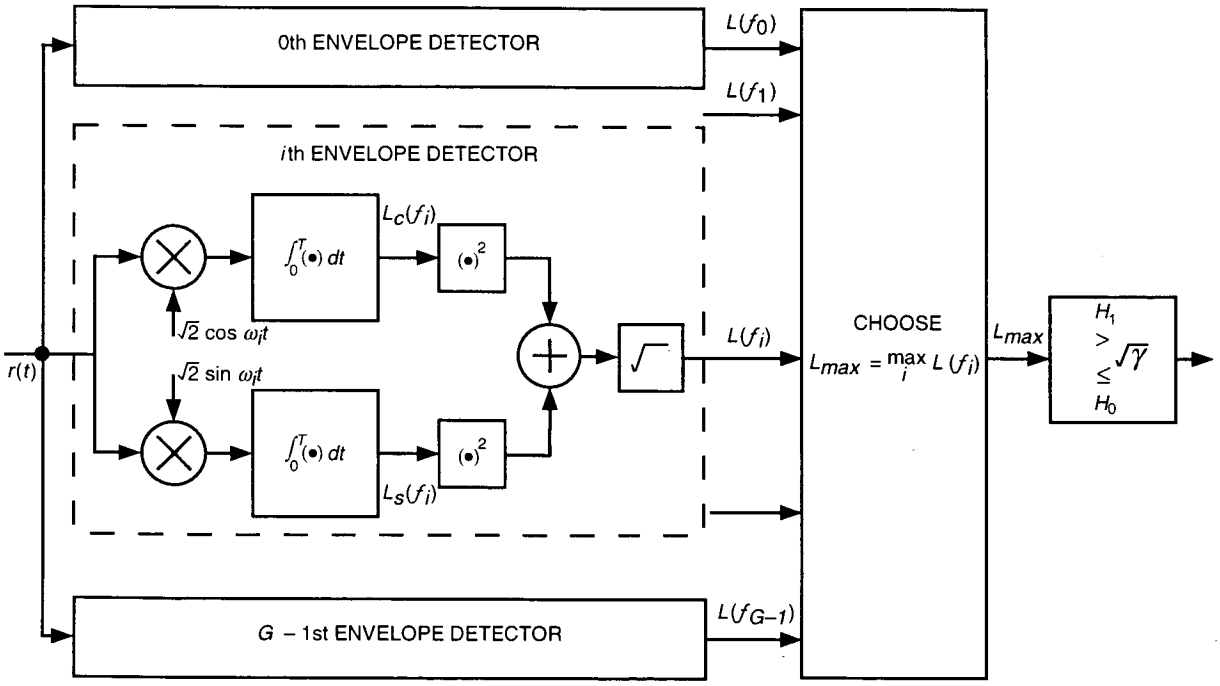

Fig. 7. Maximum-likelihood detector for detection of a single sinusoidal tone with unknown frequency and unknown phase in AWGN.

B. Performance

The performance of the MLR decision rule of Eq. (60) can be obtained analytically since the pdf of G independent random variables can be explicitly written in terms of the pdf's of individual random variables, which in turn are obtained from the results in Part 1. The procedure is as follows.

1. Best-Case Performance. Consider first the optimistic (best) case, where the actual received carrier frequency is indeed equal to one of the G frequencies, say f_k used to approximately implement the optimum decision rule as per the discussion following Eq. (59). Under $H_1, G-1$ of the $L(f_i)$'s are Rayleigh distributed with pdf [see Eq. (14)]

$$p_{L(f_i)}(L) = \frac{2}{N_0 T} L \exp\left(-\frac{L^2}{N_0 T}\right); \quad L \geq 0 \tag{61}$$

and the single $L(f_i)$ that is associated with the received signal carrier frequency, namely $L(f_k)$, is Rician distributed with pdf [see Eq. (15)]

$$p_{L(f_k)}(L) = \frac{2}{N_0 T} \exp\left(-\frac{L^2+\beta^2}{N_0 T}\right) I_0\left(\frac{2L\beta}{N_0 T}\right); \quad L \geq 0, \quad \beta^2 = PT^2 \tag{62}$$

Let P_F^* denote the *per frequency channel* false alarm probability, i.e.,

$$P_F^* = \Pr\{L(f_i) > \sqrt{\gamma} | H_0\} = \int_{\sqrt{\gamma}}^{\infty} \frac{2}{N_0 T} L \exp\left(-\frac{L^2}{N_0 T}\right) dL = \exp\left(-\frac{\gamma}{N_0 T}\right) \tag{63}$$

which is independent of f_i. Then, the overall false alarm probability, P_F, is given by

$$\begin{aligned} P_F &= \Pr\left\{\max_i L(f_i) > \sqrt{\gamma} | H_0\right\} \\ &= 1 - \Pr\{L(f_0) \leq \sqrt{\gamma}, L(f_1) \leq \sqrt{\gamma}, \cdots, L(f_{G-1}) \leq \sqrt{\gamma} | H_0\} \\ &= 1 - \prod_{i=0}^{G-1} \Pr\{L(f_i) \leq \sqrt{\gamma} | H_0\} = 1 - \prod_{i=0}^{G-1} (1 - \Pr\{L(f_i) > \sqrt{\gamma} | H_0\}) \\ &= 1 - (1 - P_F^*)^G = 1 - \left(1 - \exp\left(-\frac{\gamma}{N_0 T}\right)\right)^G \end{aligned} \tag{64}$$

Since, under H_1, $G-1$ of the spectral estimates (i.e., the ones containing noise only) have the same pdf, namely Eq. (61), as under H_0, and one spectral estimate has the Rician pdf of Eq. (62), then the overall probability of detection, P_d, is determined from

$$P_D = \Pr\left\{\max_i L(f_i) > \sqrt{\gamma} | H_1\right\} = 1 - \prod_{i=0}^{G-1} (1 - \Pr\{L(f_i) > \sqrt{\gamma} | H_1\}) = 1 - (1 - P_F^*)^{G-1} (1 - P_D^*) \tag{65}$$

where P_D^* corresponds to the detection probability of the single-frequency channel containing the signal, i.e.,

$$P_D^* = \Pr\{L(f_i) > \sqrt{\gamma} | H_1\} = Q\left(d, \sqrt{\frac{2\gamma}{N_0 T}}\right); \quad d^2 = \frac{2PT}{N_0} \tag{66}$$

Substituting Eqs. (63) and (65) into Eq. (66) gives

$$P_D = 1 - \left(1 - \exp\left(-\frac{\gamma}{N_0 T}\right)\right)^{G-1} \left(1 - Q\left(d, \sqrt{\frac{2\gamma}{N_0 T}}\right)\right) \tag{67}$$

or, equivalently, the overall probability of miss, P_M, is

$$P_M \triangleq 1 - P_D = \left(1 - \exp\left(-\frac{\gamma}{N_0 T}\right)\right)^{G-1} \left(1 - Q\left(d, \sqrt{\frac{2\gamma}{N_0 T}}\right)\right) \tag{68}$$

Note that, for $G = 1$, Eqs. (64) and (67) reduce, respectively, to Eqs. (14) and (15).

The ROC can be determined by eliminating the normalized threshold between Eqs. (64) and (67), in which case one obtains

$$P_D = 1 - (1 - P_F)^{(G-1)/G} \left(1 - Q\left(d, \sqrt{-2\ln\left(1 - (1 - P_F)^{1/G}\right)}\right)\right) \tag{69}$$

2. Worst-Case Performance. The worst-case performance occurs when the actual received carrier frequency is indeed midway between two of the G frequencies used to approximately implement the optimum decision rule as per the discussion following Eq. (59). Under H_0, the false alarm performance is still described by Eq. (64). However, under H_1, all G spectral estimates are now Rician distributed with pdf's of the form in Eq. (62), namely,

$$p_{L(f_i)}(L) = \frac{2}{N_0 T} L \exp\left(-\frac{L^2 + \beta_i^2}{N_0 T}\right) I_0\left(\frac{2L\beta_i}{N_0 T}\right); \quad L \geq 0 \tag{70}$$

where the β_i's are determined as follows. Since [see Eq. (15)]

$$\beta_i^2 \triangleq \left(E\left\{L_c(f_i)|\theta, f\right\}\right)^2 + \left(E\left\{L_s(f_i)|\theta, f\right\}\right)^2 \tag{71}$$

then, assuming that the actual received carrier frequency, f, is situated midway between f_k and f_{k+1}, which are separated by $1/T$, i.e., $f = f_k + 1/2T$, Eq. (70) is evaluated as (for simplicity, we ignore the edge effects at the ends of the frequency uncertainty band)

$$\beta_i^2 = PT^2 \left[\frac{\sin\left(\pi\left(k - i + \frac{1}{2}\right)\right)}{\pi\left(k - i + \frac{1}{2}\right)}\right]^2 = \begin{cases} PT^2\left(\frac{2}{\pi}\right)^2; & i = k, k+1 \\ PT^2\left(\frac{2}{\pi}\right)^2 \left(\frac{1}{1 + 2(k-i)}\right)^2; & i \neq k, k+1 \end{cases}$$

$$\triangleq PT^2 \Gamma_i \tag{72}$$

Finally then, analogous to Eq. (70), the detection probability would be given by

$$P_D = 1 - \prod_{i=0}^{G-1} \left(1 - Q\left(\Gamma_i d, \sqrt{\frac{2\gamma}{N_0 T}}\right)\right) \tag{73}$$

which, in general, depends on f_k, i.e., the location of f within the uncertainty band.

It has been suggested in [5] that the two nearest spectral estimates (envelopes) to the frequency location of the received signal dominate the performance, i.e., the spillover effect of signal in the other

frequency slots can be ignored to a first-order approximation. When this is done, then, under H_1, two of the spectral estimates are identically Rician distributed and the remaining $G-2$ are identically Rayleigh distributed. In this case, Eq. (73) is replaced by an expression somewhat like Eq. (67), namely,

$$P_D = 1 - \left(1 - \exp\left(-\frac{\gamma}{N_0 T}\right)\right)^{G-2} \left(1 - Q\left(\left(\frac{2}{\pi}\right) d, \sqrt{\frac{2\gamma}{N_0 T}}\right)\right)^2 \tag{74}$$

which is now independent of the frequency location of the signal. Combining Eqs. (64) and (74), the ROC is approximately given by

$$P_D = 1 - (1 - P_F)^{(G-2)/G} \left(1 - Q\left(\left(\frac{2}{\pi}\right) d, \sqrt{-2\ln\left(1 - (1 - P_F)^{1/G}\right)}\right)\right)^2 \tag{75}$$

VII. A More Precise Formulation

As discussed in Section IV of Part 1, the true transmitted signal corresponds to a sinusoidal carrier phase modulated by a square-wave subcarrier of radian frequency ω_{sc}. At the receiver, the harmonics with frequencies other than the sum and difference of ω_{sc} and ω_c are filtered out, which means that in so far as detection is concerned, the received signal in the absence of frequency uncertainty can be modeled as

$$r(t) = s(t, \theta_c, \theta_{sc}) + n(t) = \sqrt{P}\left\{\cos\left[(\omega_c + \omega_{sc})t + (\theta_c + \theta_{sc})\right] + \cos\left[(\omega_c - \omega_{sc})t + (\theta_c - \theta_{sc})\right]\right\} + n(t) \tag{76}$$

In the presence of frequency uncertainty due, for example, to Doppler shift, both the upper and lower frequency tones in Eq. (76) will be shifted from their nominal values with the higher-frequency tone experiencing a larger shift than that corresponding to the lower-frequency tone. If, however, the subcarrier frequency is much smaller than the carrier frequency, i.e., $\omega_{sc} << \omega_c$, as is the case of interest, then for all practical purposes, one can associate the frequency uncertainty with the carrier as discussed in Section V.A and assume to a first-order approximation that both upper and lower frequency tones experience the same frequency shift. Stated another way, we can assume that, in so far as detection is concerned, we observe a pair of tones whose frequencies are unknown (but by the same amount), each in a band B Hz centered around its nominal value. Furthermore, the uncertainty band is assumed to be very narrow with respect to the subcarrier frequency, i.e., $B << f_{sc}$.

A. The ALR Test

Analogous to what was done in Part 1, the conditional pdf of the received signal under hypothesis H_1 is given by

$$p(r(t)|H_1) = \left(\frac{1}{2\pi}\right)^2 \frac{1}{B} \int_{f_c - B/2}^{f_c + B/2} \int_{-\pi}^{\pi} \int_{-\pi}^{\pi} p(r(t)|H_1, \theta_+, \theta_-, f - f_{sc}, f + f_{sc}) d\theta_+ d\theta_- df \tag{77}$$

whereupon the ALR becomes

$$\Lambda(r(t)) = \exp\left\{-\frac{PT}{N_0}\right\} \frac{1}{B} \int_{f_c - B/2}^{f_c + B/2} I_0\left(\frac{\sqrt{2P}}{N_0} L_-(f)\right) I_0\left(\frac{\sqrt{2P}}{N_0} L_+(f)\right) df \tag{78}$$

In Eqs. (77) and (78), the spectral envelopes at the lower and upper tones are defined by

$$L_{\pm}(f) \triangleq \sqrt{L_{c\pm}^2(f) + L_{s\pm}^2(f)} \tag{79}$$

together with

$$\left.\begin{aligned} L_{c\pm}(f) &\triangleq \int_0^T r(t)\sqrt{2}\cos\left[2\pi(f \pm f_{sc})t\right] dt \\ L_{s\pm}(f) &\triangleq \int_0^T r(t)\sqrt{2}\sin\left[2\pi(f \pm f_{sc})t\right] dt \end{aligned}\right\} \tag{80}$$

Discretizing the integration interval results in the approximate decision rule

$$\sum_{i=0}^{G-1} I_0\left(\frac{2\sqrt{P}}{N_0}L_+(f_i)\right) I_0\left(\frac{2\sqrt{P}}{N_0}L_-(f_i)\right) \underset{H_0}{\overset{H_1}{\gtrless}} \eta \tag{81}$$

where the spectral envelopes required in Eq. (81) are defined analogously to Eqs. (79) and (80), with the continuous random variable f replaced by the discrete random variable $f_i; i = 0, 1, \cdots, G-1$. As was the case for the single-tone result in Section V.A, the performance (ROC) of the decision rule in Eq. (81) cannot be obtained analytically.

B. The MLR Test

Without going into great detail, it is straightforward to show (using the results of Section IV.B) that the MLR test analogous to Eq. (58) becomes

$$\max_f \exp\left(-\frac{PT}{N_0}\right) \exp\left(\frac{2\sqrt{P}}{N_0}L_+(f)\right) \exp\left(\frac{2\sqrt{P}}{N_0}L_-(f)\right) \underset{H_0}{\overset{H_1}{\gtrless}} \eta \tag{82}$$

or, equivalently,

$$\max_f (L_-(f) + L_+(f)) \underset{H_0}{\overset{H_1}{\gtrless}} \sqrt{\gamma} \tag{83}$$

which has the discretized version

$$\max_i (L_-(f_i) + L_+(f)) \underset{H_0}{\overset{H_1}{\gtrless}} \sqrt{\gamma} \tag{84}$$

Unfortunately, the performance of the receiver that implements the decision rule of Eq. (84) also cannot be obtained analytically.

VIII. Numerical Results

Since the performance of none of the ALR optimum decision rules can be evaluated analytically and since the same is true for some of the MLR decision rules, a computer simulation of these metrics has been developed to numerically evaluate such performance. The results of such simulations are described as follows. Figure 8 is a sample illustration of the ROC for the case of a single tone with unknown phase and frequency (as described in Section V) and a detection SNR $d^2 = 2PT/N_0 = 6$ dB. Both ALR and MLR cases are illustrated, corresponding, respectively, to the decision rules of Eqs. (54) and (60). Also, both the best- and worst-case input frequency scenarios are considered, corresponding, respectively, to the cases where the actual input frequency is indeed equal to one of the G frequencies used to approximately implement the decision rule and the case where the actual input frequency falls midway between any two of these G frequencies. Clearly, the actual system performance corresponding to an input frequency arbitrarily chosen in the uncertainty band will lie between these two performance bounds. We observe from the results in Fig. 8 that the difference between best- and worst-case performance is relatively small, as well as is the difference between the ALR (optimum) and MLR (suboptimum) decision rules. There is a significant difference, however, between the performance for $G = 10$ and $G = 100$, indicating the sensitivity of the performance degradation to a factor of 10 increase in frequency uncertainty. Also, comparing Fig. 8 with the analogous curve in Fig. 2, corresponding to the case of unknown phase but *known* frequency, we again see a rather significant degradation in performance when the frequency is unknown even by only a factor of 10 relative to the observation bandwidth (reciprocal of the observation time, T), i.e., $G = 10$.

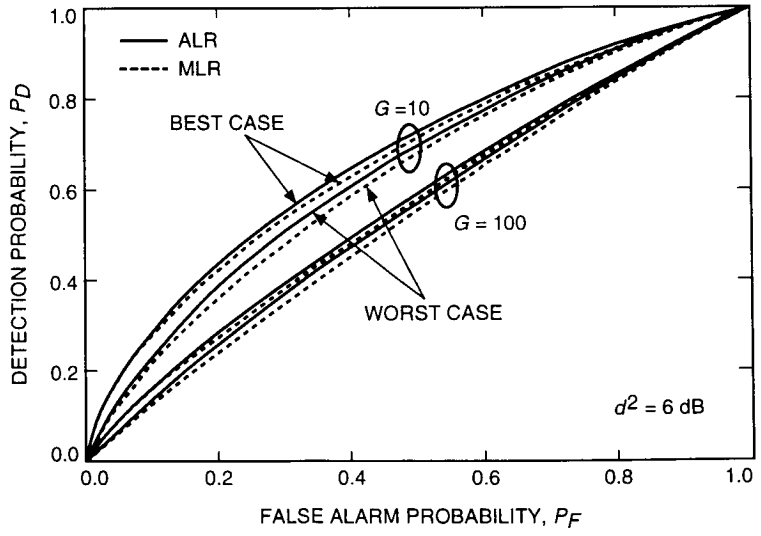

Fig. 8. ROC: frequency and phase unknown (single-tone) simulation results.

As verification of the MLR simulation results, we present in Fig. 9 the analogous analytical results obtained from Eqs. (69) and (75). Recall that in arriving at Eq. (75) the assumption was made that the energy spillover effect of the signal into the other frequency slots is dominated by the two adjacent ones. Thus, ignoring edge effects, it was not necessary to average over all possible worst-case (midway) input frequency positions. In the computer simulation, this assumption was not invoked, as the input frequency was allowed to occur midway between *any* two adjacent frequencies. Despite this analysis

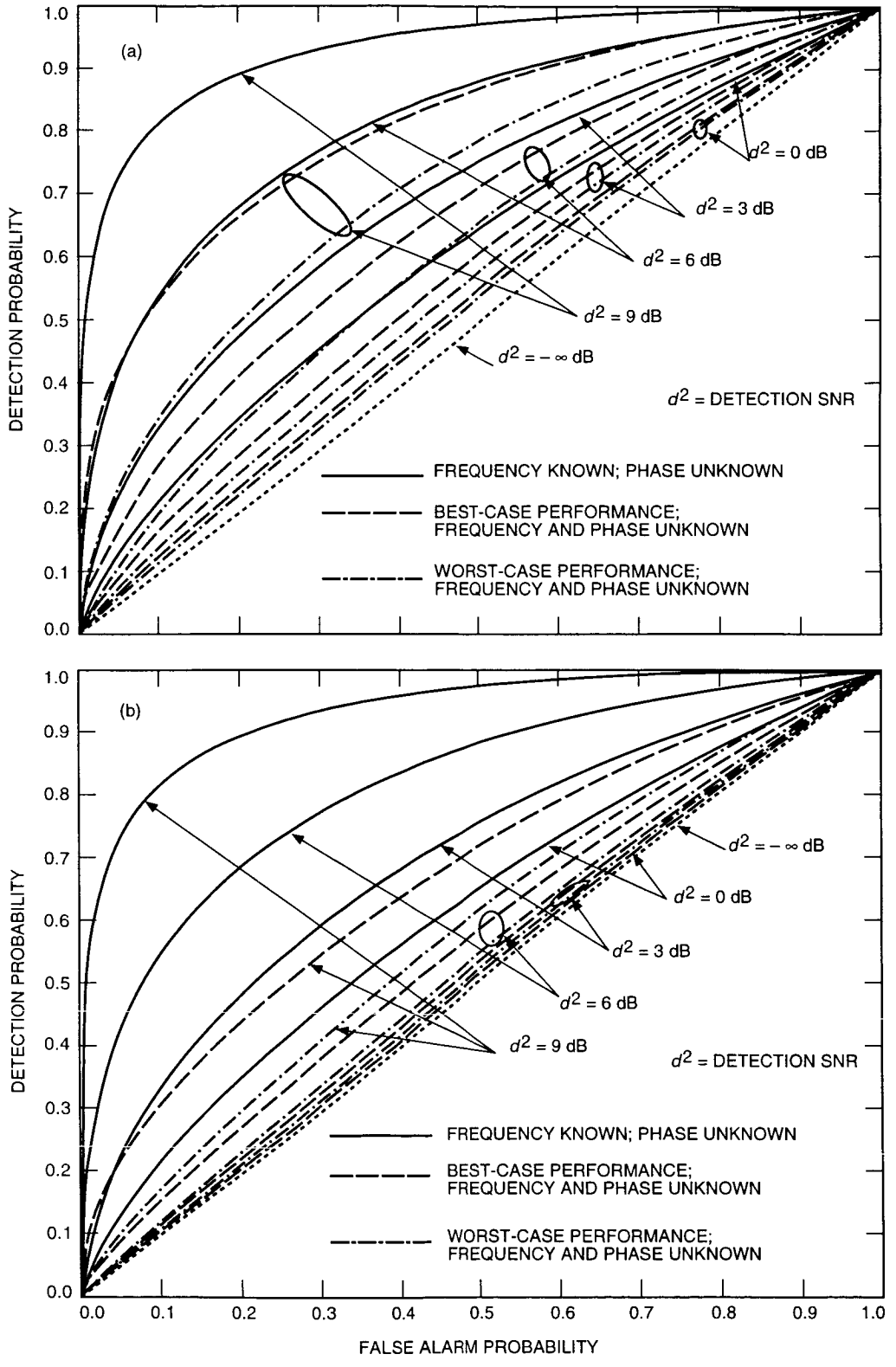

Fig. 9. ROC single tone, analytical MLR results: (a) $G = 10$ and (b) $G = 100$.

approximation, however, comparison of the results in Figs. 8 and 9 reveals excellent agreement between analysis and simulation, i.e., the assumption of only adjacent signal energy spillover used to arrive at Eq. (75) has been justified. Also indicated in Fig. 8 is the analytical result corresponding to known phase and frequency (recall that this result is the same for both MLR and ALR) that allows a more direct assessment of the performance degradation due to lack of perfect frequency knowledge.

Since the curves in Fig. 8 are drawn for a fixed value of detection SNR $d^2 = 2PT/N_0$, then assuming that P/N_0 is specified, this implies that the observation interval, T, is also held constant. Thus, changing the value of $G = BT$ from 10 to 100 directly translates into a change by a factor of 10 in the frequency uncertainty region B, which accounts for the observed degradation in performance. Another interpretation of the numerical data can be obtained by again holding P/N_0 fixed but observing the effect on system performance of increasing T for a fixed frequency uncertainty region B. This necessitates plotting the ROC with both d^2 and G increasing linearly with T. Such a plot for the ALR decision rule with best-case input frequency is illustrated in Fig. 10, where the ROC is plotted for values of $G = 10, 20, 40$, and 80 (T increasing by a factor of 2) and corresponding values $d^2 = 6, 9, 12, 15$ dB. To directly see the dependence of MLR system performance on detection SNR, Fig. 11 illustrates the behavior of detection probability, P_D, versus detection SNR, d^2, for a fixed false alarm probability, $P_F = 10^{-2}$, and values of $G = 10$ and 100. These curves are obtained from numerical evaluation of the analytical results in Section VI. Since along any curve G is held fixed, one can interpret these results as keeping the frequency uncertainty band, B, and observation time, T, fixed and observing the change in performance as P/N_0 is varied.

The penalty associated with detecting a pair of subcarrier tones (each at half the total transmitted power) as opposed to a single carrier tone (at full transmitted power) is illustrated by the numerical results in Fig. 12. Here we plot the ROC for both the single- and double-tone cases for the ALR decision rule with best-case input frequency and a detection SNR equal to 6 dB. The results for the single-tone case are taken directly from Fig. 8. We observe a significant performance penalty associated with using a double-tone detection scheme. Figure 13 illustrates for the double-tone detection scheme results analogous to Fig. 10 for the single-tone detection scheme. Here again, by comparing the two figures, we observe a significant penalty associated with using a pair of equal half-power subcarrier tones rather than a single tone at full power.

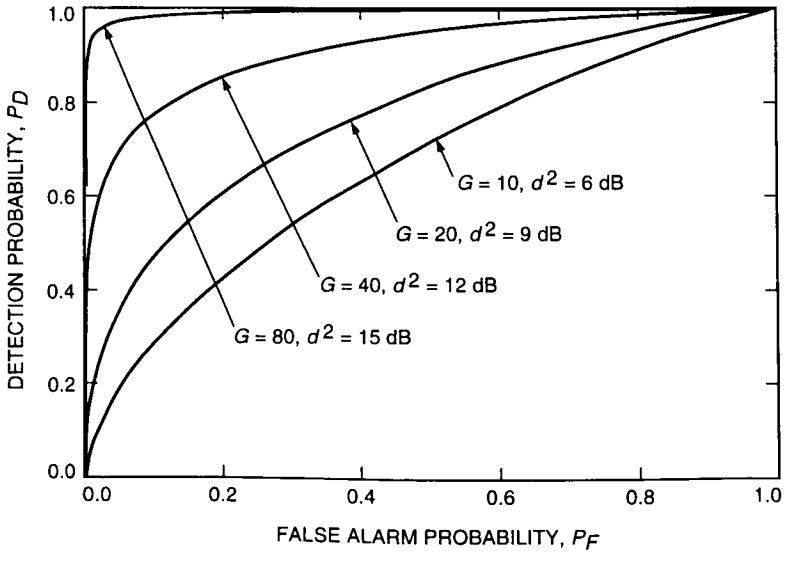

Fig. 10. ROC simulation results: frequency and phase unknown (single tone), ALR , best-case input frequency.

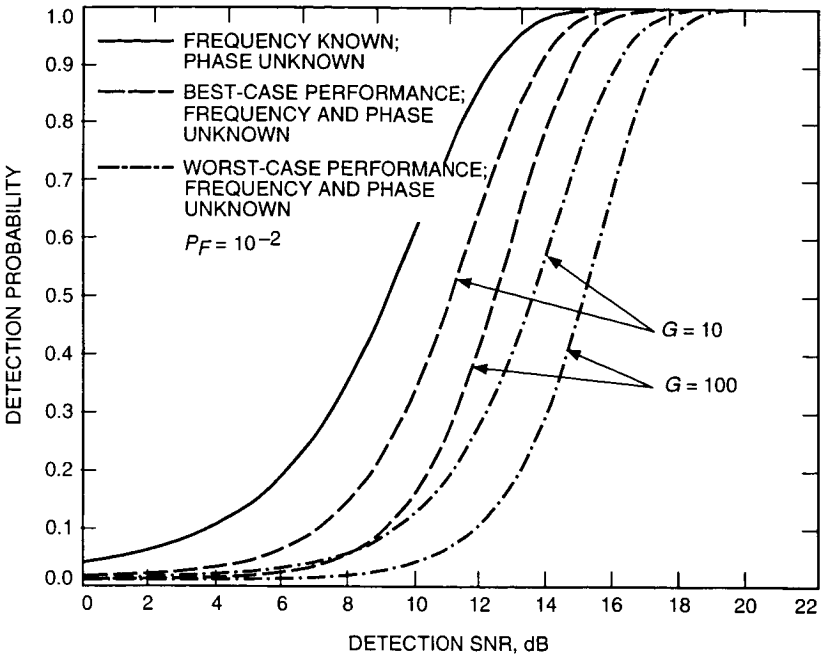

Fig. 11. Detection probability versus detection SNR analytical MLR results (single tone).

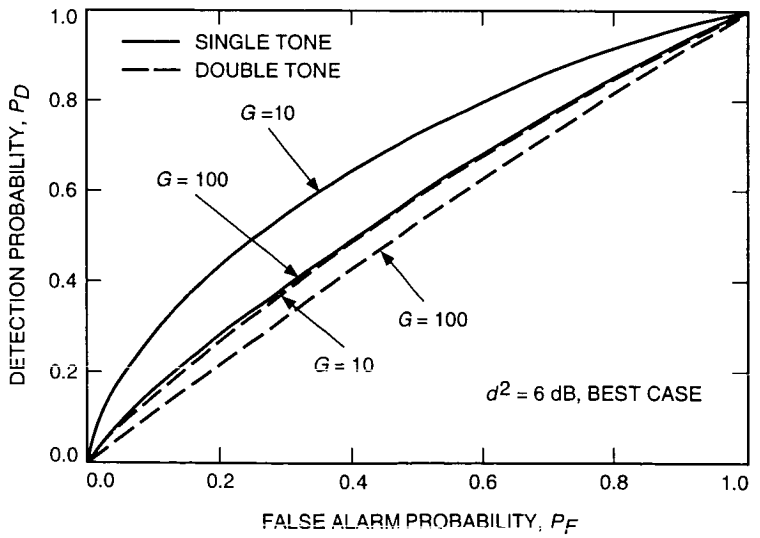

Fig. 12. ROC: frequency and phase unknown (single/double tone), ALR, best-case input frequency.

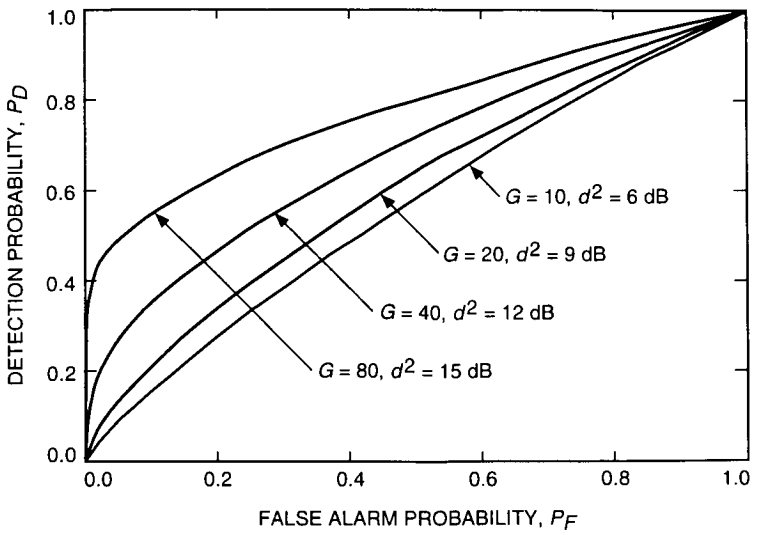

Fig. 13. ROC simulation results: frequency and phase unknown (double tone), ALR, best-case input frequency.

Acknowledgment

The authors would like to thank Mr. Van Snyder of the Supercomputing and Computational Mathematics Support Group for his advice on performing the numerical integrations required in many of the analytical results.

References

[1] H. L. VanTrees, *Detection, Estimation, and Modulation Theory, Part 1*, New York: John Wiley & Sons, Inc., 1968.

[2] M. K. Simon, S. M. Hinedi, and W. C. Lindsey, *Digital Communication Techniques: Signal Design and Detection*, Englewood Cliffs, New Jersey: Prentice-Hall, Inc., 1994.

[3] A. Polydoros and C. L. Weber, "Optimal Detection Considerations for Low Probability of Intercept," *MILCOM '82 Conference Proceedings*, Boston, Massachusetts, pp. 2.1-1–2.1-5, October 1992.

[4] A. Polydoros and K. T. Woo, "Wideband Spectral Detection of Unknown Frequency Signals," presented at the International Symposium on Information Theory, Brighton, England, June 1985.

[5] C.-D. Chung and A. Polydoros, *Multi-Hop FH/LPI Detection, Part II: Spectral Techniques*, Technical Report CSI-87-09-01, University of Southern California, Los Angeles, California, September 1987.

[6] A. Polydoros and C. L. Nikias, "Detection of Unknown-Frequency Sinusoids in Noise: Spectral Versus Correlation Detection Rules," *IEEE ASSP*, vol. 35, no. 6, pp. 897–900, June 1987.

[7] A. A. G. Requicha, "Direct Computation of Distribution Function From Characteristic Functions Using the Fast Fourier Transform," *Proceedings of the IEEE*, vol. 58, no. 7, pp. 1154–1155, July 1970.

Appendix

On the Independence of the Sum of Difference of Two Uniformly Distributed Random Variables Modulo 2π

Consider two independent random phases θ_A and θ_B that are each uniformly distributed in the semiclosed interval $[-\pi, \pi)$. Define the sum and difference of these two random variables by

$$\left.\begin{aligned} \theta'_+ &\triangleq \theta_A + \theta_B \\ \theta'_- &\triangleq \theta_A - \theta_B \end{aligned}\right\} \tag{A-1}$$

and the modulo 2π versions of these random variables by

$$\left.\begin{aligned} \theta_+ &\triangleq (\theta'_+)_{\text{mod } 2\pi} = (\theta_A + \theta_B)_{\text{mod } 2\pi} \\ \theta_- &\triangleq (\theta'_-)_{\text{mod } 2\pi} = (\theta_A - \theta_B)_{\text{mod } 2\pi} \end{aligned}\right\} \tag{A-2}$$

The probability density functions (pdf's) of θ'_+ and θ'_- are triangular in the semiclosed interval $[-2\pi, 2\pi)$, i.e., they are the convolutions of two uniform pdf's, whereas the pdf's of their modulo 2π reduced versions, θ_+ and θ_-, are once again uniformly distributed in $[-\pi, \pi)$ (see Fig. A-1). We would now like to show that θ_+ and θ_- are indeed *independent* random variables. To do this, we shall show that the conditional pdf $p_{\theta_-}(\theta_-|\theta_+)$ satisfies $p_{\theta_-}(\theta_-|\theta_+) = p_{\theta_-}(\theta_-)$, i.e., it is a uniform distribution in $[-\pi, \pi)$. Similarly, it can be shown that $p_{\theta_+}(\theta_+|\theta_-) = p_{\theta_+}(\theta_+)$.

Let θ_+ be any positive value in its region of definition, i.e., $0 \leq \theta_+ \leq \pi$. Then, θ_A and θ_B are related as follows:

$$\theta_B = \begin{cases} -\theta_A + \theta_+ - 2\pi, & -\pi < \theta_A \leq -\pi + \theta_+ \\ -\theta_A + \theta_+, & -\pi + \theta_+ \leq \theta_A \leq \pi \end{cases} \tag{A-3}$$

From Eq. (A-1), we find that

$$\theta'_- = \begin{cases} 2\theta_A - \theta_+ + 2\pi, & -\pi < \theta_A \leq -\pi + \theta_+ \\ 2\theta_A - \theta_+, & -\pi + \theta_+ \leq \theta_A \leq \pi \end{cases} \tag{A-4}$$

Thus, from Eq. (A-4) and the fact that θ_A is uniform in the interval $[-\pi, \pi)$, the conditional pdf $p_{\theta'_-}(\theta'_-|\theta_+)$ appears as in Fig. A-2(a). Reducing θ'_+ modulo 2π produces the conditional pdf $p_{\theta_-}(\theta_-|\theta_+)$ as illustrated in Fig. A-2(b), i.e., a uniform distribution in the interval $[-\pi, \pi)$ Q.E.D.

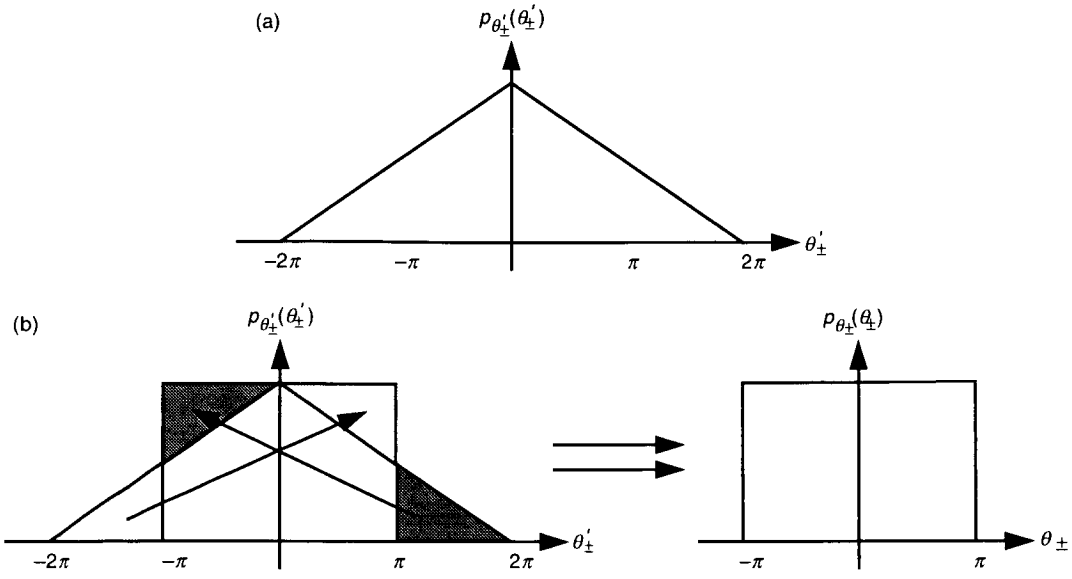

Fig. A-1. The PDF of the sum and difference of (a) two uniformly distributed random variables and (b) two uniformly distributed random variables reduced modulo 2π.

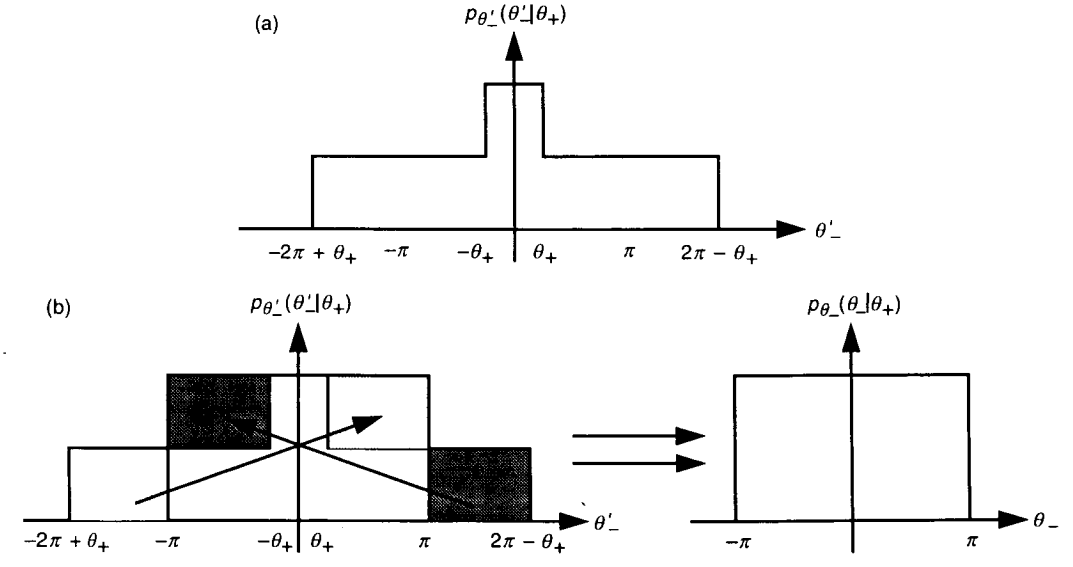

Fig. A-2. Conditional PDF of the sum and difference of (a) two uniformly distributed random variables and (b) two uniformly distributed random variables reduced modulo 2π.